

# Combined Influence of Metakaolin and Palm Oil Fuel Ash on the Heat of Hydration and Permeability of High Performance Concrete

**Mohammed A. Mansour<sup>1,2\*</sup>, Mohd Hanif Ismail<sup>1</sup>, Mohd Haziman Wan Ibrahim<sup>1</sup>, Norfaniza Mokhtar<sup>1</sup>, Abdullah Faisal Alshalif<sup>1</sup>**

<sup>1</sup> Faculty of Civil Engineering and Built Environment,  
Universiti Tun Hussein Onn Malaysia, Batu Pahat 86400, Johor, MALAYSIA

<sup>2</sup> Faculty of Engineering, Civil Engineering Department,  
Gaza University, Al Zaitoun, Gaza City, PALESTINE

\*Corresponding Author: mohdmans@gmail.com

DOI: <https://doi.org/10.30880/ijie.2025.17.05.017>

## Article Info

Received: 10 February 2024

Accepted: 4 February 2025

Available online: 30 August 2025

## Keywords

Metakaolin (MK), palm oil fuel ash (POFA), high performance concrete (HPC), heat of hydration, temperature, permeability

## Abstract

Utilizing metakaolin (MK) and palm oil fuel ash (POFA) mitigates the negative impacts of high content cement in high performance concrete (HPC). This research aims to investigate the heat of hydration (HOH) and water permeability of HPC blended with MK and POFA as cement substitutes. Three concrete mixtures namely a control made with 100% ordinary Portland cement (OPC), optimum MK; and optimum blend of MK and POFA were prepared. Subsequently, the temperature rise due to HOH and water permeability were evaluated. The results demonstrated that using 15% MK with or without 20% POFA reduced the peak temperature and coefficient of water permeability of HPC compared to control concrete. The findings suggest that incorporating MK and POFA in HPC is beneficial for mass concrete to prevent thermal cracking and for water-retaining structures to block permeable pores.

## 1. Introduction

The manufacturing of cement, especially the calcination and clinkering phases, contributes significantly to greenhouse gas emissions, particularly CO<sub>2</sub>, causing global warming. Furthermore, Cement production is energy-intensive and leads to the reduction of limestone deposits. [1]. To counter these negative consequences, strict European air pollution regulations have recommended numerous industrial by-products as supplementary cementitious materials (SCMs) [2]. Incorporating mineral admixtures to reduce cement content in HPC promotes the creation of environmentally friendly alternative materials [3].

The performance of concrete has gained increasing attention, not only for delivering high mechanical strength but also for enhancing durability and extending the life span of concrete buildings [4]. Using 100% cement adversely impacts concrete performance, leading to issues such as shrinkage and HOH [5]. Excessive cement in concrete leads to high temperature release, resulting in thermal cracking [6]. Additionally, using concrete without pozzolanic materials may not achieve high quality in resistance of the water permeability, which a significant concern for water-retaining structures and concrete exposed to chemical attack. Therefore, an effective solution is required to mitigate the heat emitted and minimize the permeability rate of concrete. Using pozzolanic materials enhances the performance of concrete, particularly in extreme environments [7]. Incorporating various pozzolans into cementitious systems modifies the reaction processes, phase compositions, microstructure development, and

overall behavior of the concrete. [8]. Pozzolanic materials, whether blended with cement or added separately, overcome the drawbacks associated with using 100% cement in HPC [9]. Moreover, adding various pozzolanic materials enhances concrete properties due to the impact of pozzolanic activity and particle fineness specific to each material [10].

Extensive research has explored the use of MK and POFA as substitutes for cement in various types of concrete. MK and POFA are regarded as highly reactive pozzolans that enhance concrete durability with their beneficial properties for HPC. The production of MK involves calcination of high purity kaolin clay at lower temperatures and resulting in lower CO<sub>2</sub> emission compared to cement [11], [12]. The unique properties of MK make it as a valuable material for enhancing concrete performance. Previous studies reported a remarkable improvement of durable and mechanical properties of concrete made with MK up to 20% as cement substitute [13], [14]. MK experienced a decrease in the temperature rise due to heat release when compared to the control concrete [15]. Nadesan et al. [16] investigated the water absorption, sorptivity and permeability of high strength self-consolidating concrete with 3.75-22.5% MK, and concluded that water transport properties were improved. On the other hand, Incorporating POFA, an agricultural waste, enhances the concrete properties in accordance to curing time, type of concrete, replacement level, chemical composition and treatment method [17], [18]. High volume of ultra-fine POFA in mortar performed more effectively than the traditional mortar in testing HOH [19]. Chandara et al. [20] concluded that the rate heat evolution and total HOH of blended cement containing ground POFA and treated POFA, decreases with increasing replacement levels. POFA helps in reducing concrete permeability as a function of the amount of cement replacement, particle fineness, and concrete age [18], [21]. Zeyad et al. [22] examined the use of ultra-fine high volumes of POFA in high strength concrete and concluded low coefficient of permeability compared to control concrete.

Recently, more focus has been given to the utilization of different pozzolanic materials in binary and ternary blends to improve the functional characteristics of concrete. This study aims to investigate the HOH and water permeability of concrete incorporating MK and POFA. The interaction between MK and POFA may significantly influence the properties of HPC when the combined mixture is properly optimized.

## 2. Materials and Methods

### 2.1 Cement and Supplementary Binders

OPC complying with BS 197 was used in the mix design for control HPC. MK and treated POFA were used as supplementary binders for modified HPC. MK was manufactured in Perak by kaolin (Malaysia) SDN BHD. The manufacturing method included calcination of kaolinite clay in a furnace at 700-750°C for 1 hour as shown in Fig. 1(a). Raw POFA was collected from the Bandung Palm Oil factory, Johor, Malaysia. The moisture of POFA was removed through a drying process in an oven at 100°C for 24 hours, then sieved through a 300- $\mu$ m mesh that were incompletely burned in the furnace. The POFA was grinded using Los Angeles machine for 8 hours to achieve finer particles. Finally, the grinded POFA was heat treated at 550°C for 1.5 hours to eliminate carbon oxide. Fig. 1(b) illustrates the treated POFA, which has a grey color. OPC, MK, and treated POFA were characterized as seen in Table 1. According to the chemical analysis using X-ray fluorescence (XRF), the total percentage of SiO<sub>2</sub>, Al<sub>2</sub>O<sub>3</sub>, and Fe<sub>2</sub>O<sub>3</sub> in MK and POFA were 94.97% and 74.91%, respectively, which qualifies them as class N and class F pozzolanic materials, respectively, per ASTM C618. MK contains a higher amount of alumina, while POFA has a higher silica content. Both MK and POFA exhibited low loss on ignition (LoI) values, in accordance with ASTM C618. From the particle size gradation, the average sizes were determined to be 16.3  $\mu$ m for OPC, 5.4  $\mu$ m for MK, and 10.6  $\mu$ m for treated POFA.



Fig. 1 Image of (a) MK (b) POFA

**Table 1** Characterization of OPC, MK and POFA

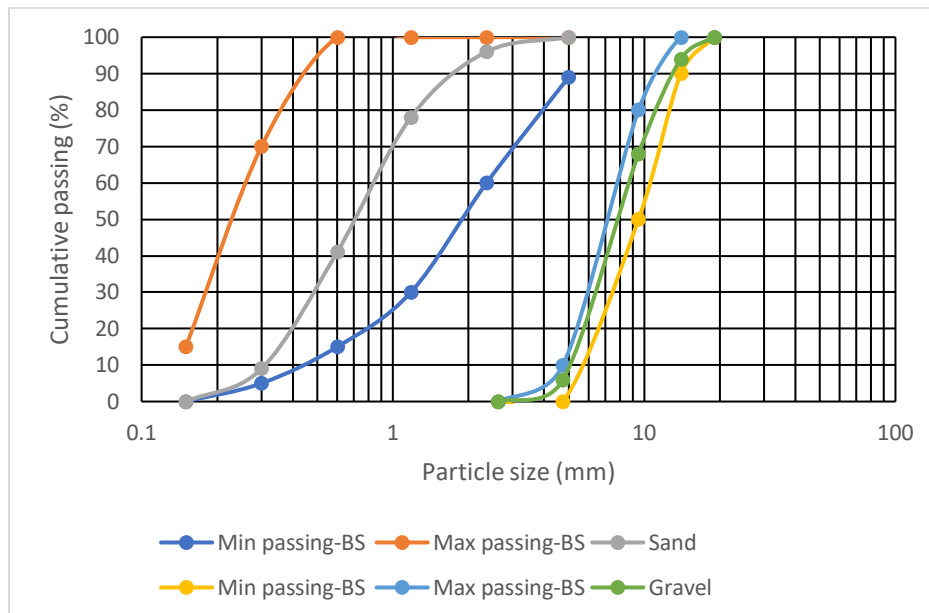
Properties	OPC (%)	MK (%)	Treated POFA (%)
<b>Oxides composition</b>			
SiO <sub>2</sub>	20.63	54.04	62.26
Al <sub>2</sub> O <sub>3</sub>	4.71	40.33	6.96
Fe <sub>2</sub> O <sub>3</sub>	3.52	0.60	5.69
CaO	61.65	0.03	8.19
MgO	0.97	0.19	4.18
Na <sub>2</sub> O	0.06	-	4.10
K <sub>2</sub> O	1.08	2.32	5.39
SO <sub>3</sub>	4.98	-	0.22
LOI	2.40	2.49	3.01
SiO <sub>2</sub> +Al <sub>2</sub> O <sub>3</sub> +Fe <sub>2</sub> O <sub>3</sub>	28.86	94.97	74.91
<b>Physical parameters</b>			
Specific gravity	3.15	2.54	2.23
Specific surface area (cm <sup>2</sup> /g)	5267	16156	13275
Median particle size (μm)	16.3	5.4	10.6
color	Grey	White	Grey

## 2.2 Fine and Coarse Aggregates

River sand with a maximum size of 5 mm was used as fine aggregate and gravel with a maximum size of 12.5 mm was used as coarse aggregate. Fig. 2 presents the sieve analysis performed to evaluate the grading of fine and coarse aggregates, confirming that the particle size distribution meets standard requirements according to BS 410. This ensures that the aggregates are well-graded, promoting denser concrete mix and minimizing voids. The coarse aggregates utilized in this study were clean, free from detrimental coatings of dust and clay. Sand and gravel were kept in a dry condition to ensure that moisture content did not affect the mixture. Fine and coarse aggregates underwent testing for specific gravity, unit weight, and water absorption as seen in Table 2.

**Table 2** Physical properties of fine and coarse aggregates

Aggregate	Specific gravity	Unit weight (kg/m <sup>3</sup> )	Water absorption (%)
Fine aggregate	2.59	1453	0.97
Coarse aggregate	2.62	1481	0.86

**Fig. 2** Fine and coarse aggregates sieve analysis

## 2.3 Mix Proportion and Specimens Preparation

The trial mix approach was employed to determine proportions for HPC. To achieve high strength, a low water to cement ratio (0.27) and a high OPC content were used. For the control mixture, the mix proportions used throughout this study for OPC, fine aggregate and coarse aggregate were 1:1.35:1.88, respectively. A high-water reducing admixture classified polymer-based superplasticizer was added to keep the concrete workable. Table 3 outlines the mix proportions of HPC specimens. Small amounts of materials were added in sequence during the batching procedure to prevent the mix from balling until the batch became homogeneous. Cubes with dimensions of 100 mm were used for compressive strength tests at ages of 7 and 28 days. For HOH, cylinders with dimensions  $\phi 100 \times 200$  mm were used to evaluate the temperature rise of pre-hardened concrete. For the water permeability test, Cubes with dimensions of 150 mm were used at ages of 28, 56 and 90 days.

The optimum MK and optimum combined MK and POFA was evaluated via the compressive strength. First, the optimum MK proportion was evaluated by testing three percentages: 5%, 10%, and 15% as cement replacements. The optimal finding from the HPC blended with MK was selected to evaluate the optimum blend of MK and POFA. Three percentages of POFA: 20%, 30%, and 40% as cement replacements was combined with the optimum MK percentage calculated earlier to obtain the optimum blend of MK and POFA. The control HPC and the optimum specimens were then subjected to HOH and water permeability tests.

**Table 3** Mix proportion of HPC

Mixture	OPC (kg)	MK	POFA	Fine Agg. (kg)	Coarse Agg. (kg)	w/c	SP (kg)
Control	550	-	-	743	1034	0.27	11
HPC blended with MK							
Optimum	M5	522.5	5%	-	743	1034	0.27
MK	M10	495	10%	-	743	1034	0.27
	M15	467.5	15%	-	743	1034	0.27
HPC blended with MK and POFA							
Optimum	OptMP20	Was found later	Optimum	20%	743	1034	0.27
MKPOFA	OptMP30	Was found later	Optimum	30%	743	1034	0.27
	OptMP40	Was found later	Optimum	40%	743	1034	0.27

w/c is water/cement ratio and SP is superplasticizer

## 3. Testing Program

### 3.1 Compressive Strength

The compressive strength test was used to determine the optimal samples at 7 and 28 days. The test followed BS 12390-3, utilizing an automatic compression machine with a 3000 kN capacity and a loading rate of 7 kN/s.

### 3.2 Measurement of Hydration Temperature

The temperature rise due to the HOH was measured for HPC samples. Fig. 3 shows the experimental setup for measuring the temperature of concrete. A polystyrene cube with dimensions 400×400×400 mm was used as an external insulator. To improve the insulation of the concrete, extra polystyrene was added inside the cube and shaped to match the PVC cylinder ( $\phi 100 \times 200$  mm). A Type K thermocouple was promptly inserted through the box cover into the centre of the cylinder as soon as the concrete was poured. The thermocouple was linked to a computer-controlled data logging device. The heat was released during the hydration reaction as the HPC was poured into the PVC cylinder, resulting in an increase in hydration temperature. Concrete temperature readings were recorded at one-hour intervals over a period 120 hours. After the PVC cylinders were placed inside the polystyrene cube immediately following mixing, the concrete temperature initially increased and then gradually decreased to values close to the initial reading.

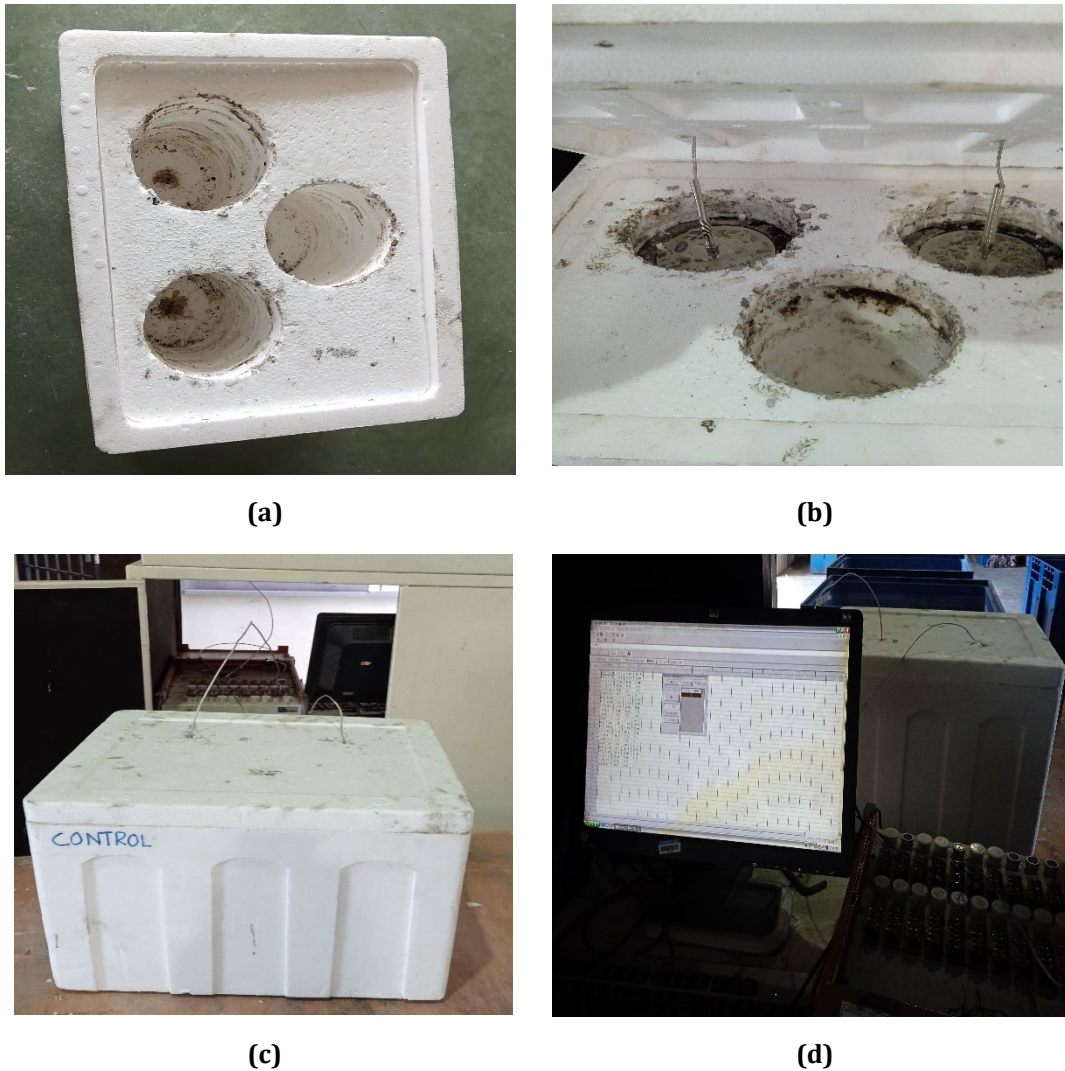


Fig. 3 Temperature of HOH arrangement test

### 3.3 Water Permeability

The permeability of concrete was tested in accordance to BS EN 12390-8: 2009. Concrete cubes with 150 mm sides were placed on water permeability equipment, ensuring a smooth surface. A water pressure of 5-bar was applied for 72 hours, as illustrated in Fig. 4(a). Afterward, the specimens were weighed and then split along the plane perpendicular to the surface where the pressure was applied. The depth of water penetration was accurately marked, as depicted in Fig. 4(b). The coefficient of permeability was calculated according to Valenta's Eqn. 3.1 [23].

$$K = \frac{vd^2}{2ht} \quad (1)$$

$$v = \frac{m}{Ad\rho} \quad (2)$$

where  $K$  is the coefficient of water permeability (m/s),  $v$  is the porosity of concrete,  $d$  is the depth of water penetration (m),  $h$  is the hydraulic head (m), and  $t$  is the time under pressure (s),  $m$  is the gain in mass (kg),  $A$  is the cross-section area (mm<sup>2</sup>), and  $\rho$  is the density of water.



Fig. 4 Water permeability test

## 4. Findings and Discussion

### 4.1 Compressive Strength

The sections below discuss the compressive strength findings of substituting cement with MK and POFA to create the following mixtures: optimum MK and optimum blend of MK and POFA.

#### 4.1.1 Optimum Compressive Strength of HPC Blended with MK

The compressive strength of HPC with MK replacing 5%, 10%, and 15% of the cement was consistently higher than that of the control HPC, as seen in Fig. 5. The optimal compressive strength was achieved at a 15% ratio of MK replacement with values of 69.9 MPa and 81.8 MPa at 7 and 28 days, respectively. This can be attributed to the pore-filling effect and pozzolanic reactivity of fine MK particles. Due to the high pozzolanic reactivity of MK, its reaction with portlandite improved the compressive strength of HPC. [24]. Most studies have shown that the incorporation of MK in the range of 10-15% had satisfactorily enhanced the compressive strength of concrete. This aligns with the findings of Zhang et al. [25] and Izadifard et al. [26], found that 15% is the optimal level of MK for achieving the highest compressive strength.

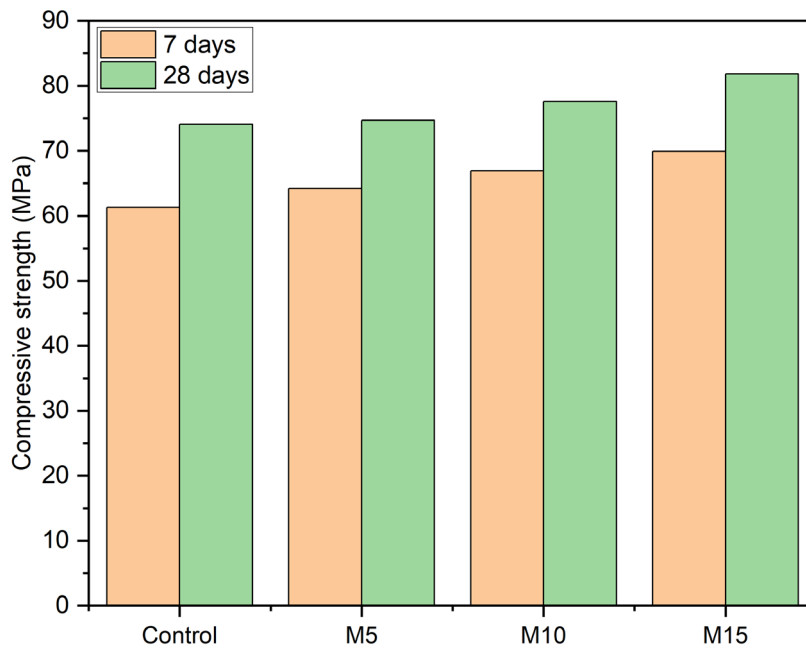


Fig. 5 Compressive strength of HPC blended with MK

#### 4.1.2 Optimum Compressive Strength of HPC with Blend of MK and POFA

Fig. 6 presents the compressive strength of combined MK and POFA. The compressive strength of combined 15% MK and 20% POFA with values of 62.8 and 75.6 MPa at ages of 7 and 28 days, respectively and marginally surpassed the control HPC. The addition of MK and POFA to HPC leads to pozzolanic enhancement, reduction of the concrete porosity, and the reduction of permeable voids [15]. Silica present in MK and POFA reacts with portlandite to form tobermorite, thereby strengthening the concrete matrix [11], [27]. It is observed that incorporation MK in HPC increases the early-age strength of concrete, while POFA has no significant effect during this stage.

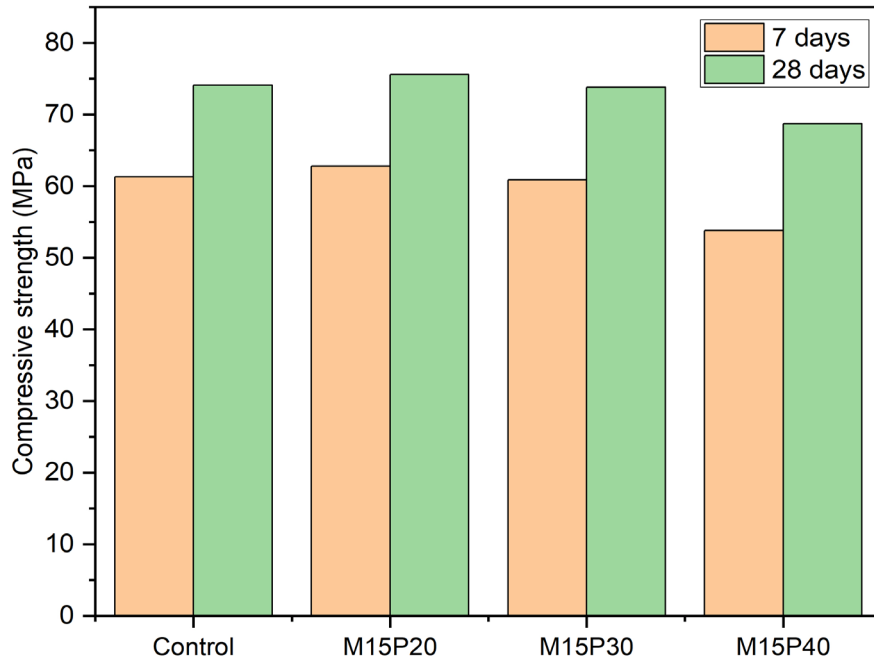


Fig. 6 Compressive strength of HPC blended with both MK and POFA

#### 4.2 Evaluation of Hydration Temperature

Fig. 7 illustrates the temperature data over time for the control HPC, M15 and M15P20. The peak temperature and the time to reach it typically varied for the mixtures after concrete placement. Finally, the temperature reached stable values to some extent during the later stages of testing. Table 3 presents the temperature data of HPC mixtures. The starting temperatures of M15 and M15P20 mixtures were lower compared to the control HPC. M15 achieved the lowest peak temperature of 38.35°C at 19 hours after casting, whereas the control HPC reached the highest peak temperature of 41.2°C at 20 hours after casting. The control HPC, composed of 100% OPC, experienced a high hydration temperature due to its high cement content [28]. The hydration of cement particles resulted in rapid initial hydration, leading to an uneven distribution of cement paste and a weak structure. Although MK and POFA have a higher surface area, the hydration temperature did not increase, verifying the retarding effect that reduces the HOH in concrete. This agrees with Barkat et al. [15] stating that increasing MK in mortar decreases the temperature rise. According to Mansour et al [29] incorporation 5-15 % MK in high strength concrete reduced the hydration temperature compared to the conventional mixture. For concrete blended with POFA, Abdul Awal et al. [30] observed a reduction of HOH in concrete containing 30% POFA.

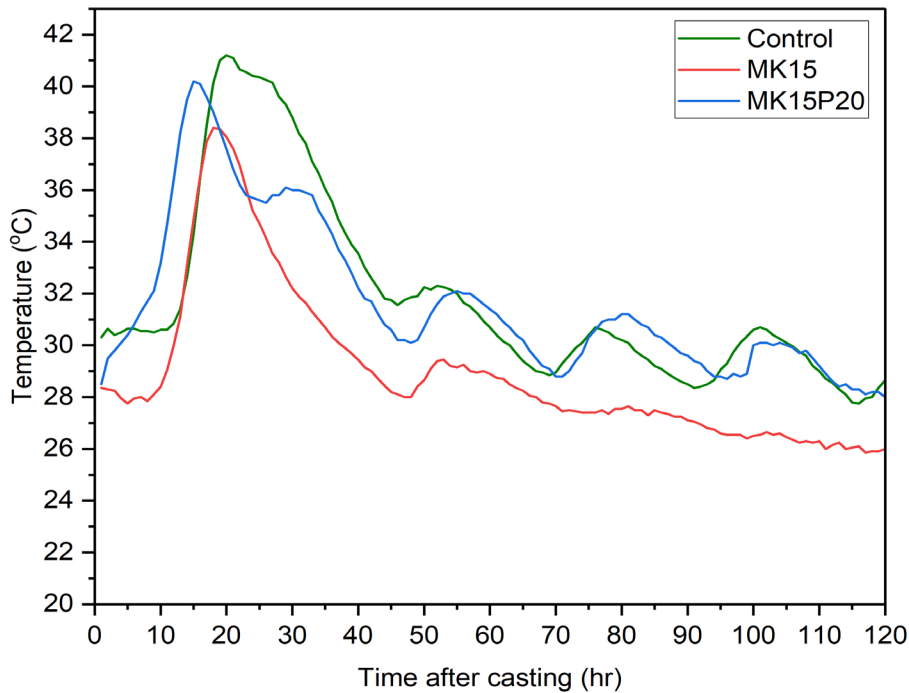


Fig. 7 Evolution of hydration temperature of concrete mixtures

Table 4 Temperature characteristics of concrete mixtures

	Control HPC	M15	M15P20
Initial temperature	30.3 °C	28.4 °C	28.5 °C
Peak temperature	41.2 °C	38.4 °C	40.2 °C
Time to reach peak temperature	20 hrs	19 hrs	16 hrs
Average ambient temperature	28.2 °C	25.4 °C	28.7 °C

The basic factors influencing the temperature rise of concrete are materials and the dimensions of concrete element. Other factors influencing temperature rise are ambient temperature, casting period, formwork and cooling system [31]. Superplasticizer did not significantly affect the heat release in HPC [32]. Nevertheless, the time to reach the peak temperature is increased by high ratios of superplasticizer [33]. Despite using the same ratio of superplasticizer (2%) for the control, M15 and M15P20 mixtures, the time to reach the peak temperature varied among them. M15P20 recorded a reduction in the time to reach peak temperature (16 hours) compared to control sample (20 hours). Increasing the ratio of MK and POFA in concrete enhance the uptake of superplasticizer thus reducing the time to reach the peak temperature. The excess superplasticizer in concrete causes retardation of hydration and delay of setting time [34].

### 4.3 Water Permeability

Fig. 8 illustrates that the incorporation of MK and POFA reduced the water permeability of HPC. The depth of water penetration tests recorded 20.4 mm, 15.3 mm and 12.5 mm at the age of 28 days; and 17.6, 13.5 and 11.6 mm at the age of 90 days for control HPC, M15 and M15P20, respectively. Referring to the Table 5, the coefficient of permeability tests recorded  $2.798 \times 10^{-12}$  m/s,  $2.099 \times 10^{-12}$  m/s and  $1.715 \times 10^{-12}$  m/s at age of 28 days; and  $1.811 \times 10^{-12}$  m/s,  $1.389 \times 10^{-12}$  m/s and  $1.392 \times 10^{-12}$  m/s at age of 90 days for control HPC, M15 and M15P20 at age of 90 days, respectively. The formation of fine C-S-H gel helps blocks the pores within the matrix, leading to a reduction in concrete porosity. This is in line with the findings of Nadesan & Dinakar [16] who investigated incorporating 3.75-22.5% MK in high strength concrete and found that 15% MK was the optimum ratio for reducing water permeability. According to the influence of POFA on permeability, Zeyad et al. [35] stated that adding 20-60% POFA in high strength concrete minimizes coefficient of permeability and Sanawung et al. [21] observed increasing POFA 15-35% in concrete decreases the permeability rate.

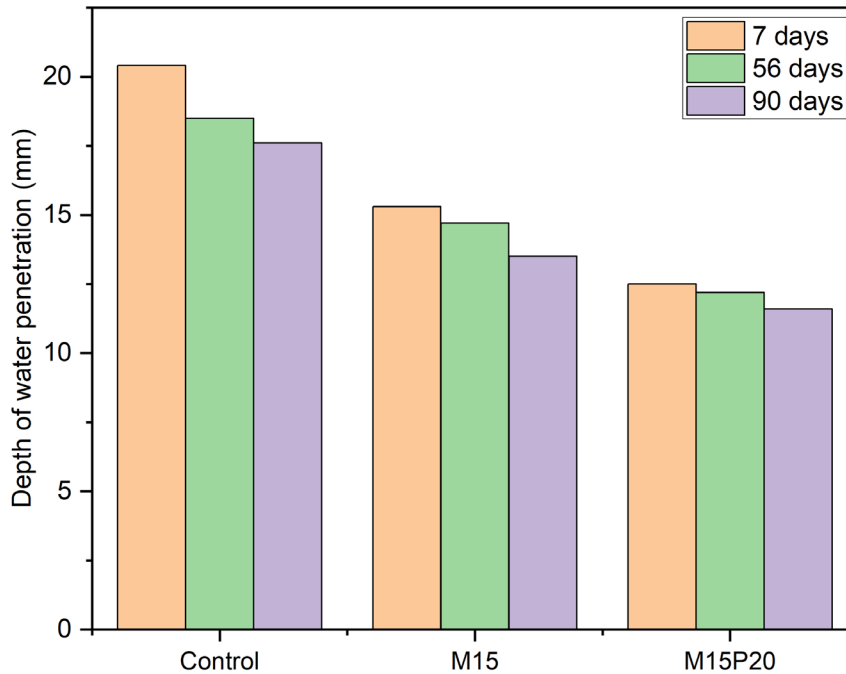


**Fig. 8** Depth of water penetration of concrete mixtures

**Table 5** Coefficient of permeability of concrete mixtures

Mixture	Age (days)	Depth of water penetration (mm)	Coefficient of permeability (m/s)
Control	28	20.4	$2.798 \times 10^{-12}$
	56	18.5	$2.221 \times 10^{-12}$
	90	17.6	$1.811 \times 10^{-12}$
M15	28	15.3	$2.099 \times 10^{-12}$
	56	14.7	$1.764 \times 10^{-12}$
	90	13.5	$1.389 \times 10^{-12}$
M15P20	28	12.5	$1.715 \times 10^{-12}$
	56	12.2	$1.646 \times 10^{-12}$
	90	11.6	$1.392 \times 10^{-12}$

## 5. Conclusion

The role of MK and POFA in affecting the HOH and permeability of HPC was emphasized. Based on the experimental findings, the following conclusions were reached.

- HPC with 15% MK replacing OPC achieved the highest strength throughout the curing period. Therefore, MK is considered a competitive alternative to traditional SCMs for use in HPC. The combination of 15% MK and 20% POFA achieved the highest compressive strength among the hybrid blends of MK and POFA.
- The inclusion of MK and POFA leads to reduction of temperature rise of HPC. Particularly, MK blended HPC was effective in reducing HOH. MK and POFA lower the build-up of heat inside the concrete core; eventually, the internal temperature and thermal gradients of mass concrete are lowered, preventing thermal cracking.
- MK and POFA played a significant role in reducing the water permeability of concrete. The results of the depth of water penetration indicated values less than 25 mm, which is the recommended value when considering the durability of concrete, specifically in concrete used for water-retaining structures and exposed to chemical attack.
- Overall, the suggested HPC incorporating MK and POFA is less polluting, energy-saving and more durable than the conventional HPC. Utilization of sustainable materials as cement replacements in HPC could be promoted in the construction industry to mitigate the environmental impact of the increased use of cement.

- Further experiments for HPC with MK and POFA are required to assess abrasion, toughness, impact resistance and freeze-thaw.

## Acknowledgement

This study was funded by the Ministry of Higher Education (MOHE) through the Fundamental Research Grant Scheme (FRGS/1/2021/STG05/UTHM/03/2). The authors extend their gratitude to the staff of Universiti Tun Hussein Onn's Faculty of Civil Engineering and Built Environment laboratory, where the research was carried out, and to Bandung Palm Oil Mill Sdn. Bhd.

## Conflicts of Interest

Authors declare that there is no conflict of interests regarding the publication of the paper.

## Author Contribution

The authors confirm contribution to the paper as follows: **study conception and design:** Mansour M, Hanif M; **data collection:** Mansour M; **analysis and interpretation of results:** Haziman M, Mokhtar N, Alsharif A; **draft manuscript preparation:** Mansour M, Hanif M. All authors reviewed the results and approved the final version of the manuscript.

## References

- [1] Odeyemi, S.O., Abdulwahab, R., Giwa, Z. T., Anifowose, M. A., Odeyemi, O. T. & Ezenweani, C. F. (2021) Effect of combining maize straw and palm oil fuel ashes in concrete as partial cement replacement in compression, *Trends in Sciences*, 18, 1–11, <https://doi.org/10.48048/tis.2021.29>
- [2] Gyurkó, Z., Szijártó, A. & Nemes, R. (2019) Cellular concrete waste as an economical alternative to traditional supplementary cementitious materials, *Journal of Thermal Analysis and Calorimetry*, 138, 947–61, <https://doi.org/10.1007/s10973-019-08303-8>
- [3] Mansour, M. A., Ismail, M. H. Bin, Imran Latif, Q. B. alias, Alsharif, A.F., Milad, A. & Bargi, W.A. Al. (2023) A Systematic Review of the Concrete Durability Incorporating Recycled Glass, *Sustainability (Switzerland)*, 15, <https://doi.org/10.3390/su15043568>
- [4] Shi, W. & Shafei, B. (2021) Bond characteristics between conventional concrete and six high-performance patching materials, *Construction and Building Materials*, Elsevier Ltd. 308, 124898, <https://doi.org/10.1016/j.conbuildmat.2021.124898>
- [5] Kannan, D. M., Aboubakr, S. H., EL-Dieb, A. S. & Reda Taha, M. M. (2017) High performance concrete incorporating ceramic waste powder as large partial replacement of Portland cement, *Construction and Building Materials*, 144, 35–41, <https://doi.org/10.1016/j.conbuildmat.2017.03.115>
- [6] Wei, J. (2017) Impact of Cement Hydration on Durability of Cellulosic Fiber-Reinforced Cementitious Composites in the Presence of Metakaolin, *Advanced Engineering Materials*, 20, 1–12, <https://doi.org/10.1002/adem.201700642>
- [7] Satyanarayana, G. V. V. & Chaitanya, B. K. (2019) Durability properties of m60 gradeself-compacting concrete with partial replacement of cement by GGBS, lime powder and metakaolin, *International Journal of Recent Technology and Engineering*, 8, 7717–20, <https://doi.org/10.35940/ijrte.C6289.098319>
- [8] Sujjavanich, S., Suwanvitaya, P., Chaysuwan, D. & Heness, G. (2017) Synergistic effect of metakaolin and fly ash on properties of concrete, *Construction and Building Materials*, Elsevier Ltd. 155, 830–7, <https://doi.org/10.1016/j.conbuildmat.2017.08.072>
- [9] Çiflikli, M., Sarıdemir, M. & Soysat, F. (2018) Adverse effects of high temperatures and freeze-thaw cycles on properties of HFRHSCs containing silica fume and metakaolin, *Construction and Building Materials*, 174, 507–19, <https://doi.org/10.1016/j.conbuildmat.2018.04.150>
- [10] Dembovska, L., Bajare, D., Pundiene, I. & Vitola, L. (2017) Effect of Pozzolanic Additives on the Strength Development of High Performance Concrete, *Procedia Engineering*, 172, 202–10, <https://doi.org/10.1016/j.proeng.2017.02.050>
- [11] Ashish, D. K. & Verma, S. K. (2019) Cementing Efficiency of Flash and Rotary-Calcined Metakaolin in Concrete. *Journal of Materials in Civil Engineering*, 31, 04019307, [https://doi.org/10.1061/\(asce\)mt.1943-5533.0002953](https://doi.org/10.1061/(asce)mt.1943-5533.0002953)
- [12] Gill, A. S. & Siddique, R. (2018) Durability properties of self-compacting concrete incorporating metakaolin and rice husk ash. *Construction and Building Materials*, Elsevier Ltd., 176, 323–32, <https://doi.org/10.1016/j.conbuildmat.2018.05.054>

- [13] Danish, P. & Mohan Ganesh, G. (2020) Durability properties of self-compacting concrete using different mineral powders additions in ternary blends, *Revista Romana de Materiale/ Romanian Journal of Materials*, 50, 369–78.
- [14] Xupeng, C., Zhuowen, S. & Jianyong, P. (2021) Effects of active mineral admixture on mechanical properties and durability of concrete. *Materials Research Express*, IOP Publishing, 8, 115506, <https://doi.org/10.1088/2053-1591/ac3b7e>
- [15] Barkat, A., Kenai, S., Menadi, B., Kadri, E. & Soualhi, H. (2019) Effects of local metakaolin addition on rheological and mechanical performance of self-compacting limestone cement concrete, *Journal of Adhesion Science and Technology*, Taylor & Francis, 33, 963–85, <https://doi.org/10.1080/01694243.2019.1571737>
- [16] Nadesan, M. S. & Dinakar, P. (2017) Permeation properties of high strength self-compacting and vibrated concretes. *Journal of Building Engineering*, Elsevier Ltd., 12, 275–81, <https://doi.org/10.1016/j.jobe.2017.06.003>
- [17] Kamaruddin, S., Goh, W. I., Abdul Mutalib, N. A. N., Jhatial, A. A., Mohamad, N. & Rahman, A. F. (2021) Effect of Combined Supplementary Cementitious Materials on the Fresh and Mechanical Properties of Eco-Efficient Self-Compacting Concrete, *Arabian Journal for Science and Engineering*, Springer Berlin Heidelberg, 46, 10953–73, <https://doi.org/10.1007/s13369-021-05656-x>
- [18] Khankhaje, E., Hussin, M. W., Mirza, J., Rafieizonooz, M., Salim, M. R., Siong, H. C. et al. (2016) On blended cement and geopolymer concretes containing palm oil fuel ash. *Materials and Design*, 89, 385–98, <https://doi.org/10.1016/j.matdes.2015.09.140>
- [19] Lim, N. H. A. S., Ismail, M. A., Lee, H. S., Hussin, M. W., Sam, A. R. M. & Samadi, M. (2015) The effects of high volume nano palm oil fuel ash on microstructure properties and hydration temperature of mortar, *Construction and Building Materials*, 93, 29–34, <https://doi.org/10.1016/j.conbuildmat.2015.05.107>
- [20] Chandara, C., Mohd Azizli, K.A., Ahmad, Z.A., Saiyid Hashim, S.F. & Sakai, E. (2012) Heat of hydration of blended cement containing treated ground palm oil fuel ash. *Construction and Building Materials*, Elsevier Ltd. 27, 78–81, <https://doi.org/10.1016/j.conbuildmat.2011.08.011>
- [21] Sanawung, W., Cheewaket, T., Tangchirapat, W. & Jaturapitakkul, C. (2017) Influence of Palm Oil Fuel Ash and W/B Ratios on Compressive Strength, Water Permeability, and Chloride Resistance of Concrete, *Advances in Materials Science and Engineering*, <https://doi.org/10.1155/2017/4927640>
- [22] Zeyad, A. M., Megat Johari, M. A., Tayeh, B. A. & Yusuf, M. O. (2017) Pozzolanic reactivity of ultrafine palm oil fuel ash waste on strength and durability performances of high strength concrete, *Journal of Cleaner Production*, 144, 511–22, <https://doi.org/10.1016/j.jclepro.2016.12.121>
- [23] Liu, X. & Zhang, M. H. (2010) Permeability of high-performance concrete incorporating presoaked lightweight aggregates for internal curing. *Magazine of Concrete Research*, 62, 79–89, <https://doi.org/10.1680/macr.2008.62.2.79>
- [24] Raheem, A. A., Abdulwahab, R. & Kareem, M. A. (2021) Incorporation of metakaolin and nanosilica in blended cement mortar and concrete- A review, *Journal of Cleaner Production*, 290, 125852, <https://doi.org/10.1016/j.jclepro.2021.125852>
- [25] Zhang, S., Zhou, Y., Sun, J. & Han, F. (2021) Effect of ultrafine metakaolin on the properties of mortar and concrete, *Crystals*, 11, <https://doi.org/10.3390/cryst11060665>
- [26] Izadifard, R. A., Abdi Moghadam, M. & Sepahi, M. M. (2021) Influence of metakaolin as a partial replacement of cement on characteristics of concrete exposed to high temperatures, *Journal of Sustainable Cement-Based Materials*, Taylor & Francis, 10, 336–52, <https://doi.org/10.1080/21650373.2021.1877206>
- [27] Chand, G., Happy, S. K. & Ram, S. (2021) Assessment of the properties of sustainable concrete produced from quaternary blend of portland cement, glass powder, metakaolin and silica fume, *Cleaner Engineering and Technology*, 4, 100179, <https://doi.org/10.1016/j.clet.2021.100179>
- [28] Kim, G., Lee, E. & Koo, K. (2009) Hydration heat and autogenous shrinkage of high-strength mass concrete, *Journal of Asian Architecture and Building Engineering*, 8, 509–18, <https://doi.org/10.3130/jaabe.8.509>
- [29] Mansour, M. A., Ismail, M.H., Majid, M. A., Noor, N. M. & Deraman, R. (2023) Compressive Strength, Temperature Performance and Shrinkage of Concrete Containing Metakaolin, *International Journal of Integrated Engineering*, 15, 126–34, <https://doi.org/10.30880/IJIE.2023.15.06.014>
- [30] Abdul Awal, A. S. M. & Warid Hussin, M. (2011) Effect of palm oil fuel ash in controlling heat of hydration of concrete. *Procedia Engineering*, 14, 2650–7, <https://doi.org/10.1016/j.proeng.2011.07.333>

- [31] Schackow, A., Effting, C., Gomes, I. R., Patruni, I. Z., Vicenzi, F. & Kramel, C. (2016) Temperature variation in concrete samples due to cement hydration, *Applied Thermal Engineering*, 103, 1362–1369. <https://doi.org/10.1016/j.applthermaleng.2016.05.048>
- [32] Bourchy, A., Barnes, L., Bessette, L., Chalencou, F., Joron, A. & Torrenti, J. M. (2019) Optimization of concrete mix design to account for strength and hydration heat in massive concrete structures, *Cement and Concrete Composites*, 103, 233–41, <https://doi.org/10.1016/j.cemconcomp.2019.05.005>
- [33] Jaskulski, R., Kubissa, W. & Prałat, K. (2019) Influence of PCP Based Superplasticizer on Heat Emission during Portland Cement Hydration, *IOP Conference Series: Materials Science and Engineering*, 661, <https://doi.org/10.1088/1757-899X/661/1/012139>
- [34] Šiler, P., Kolářová, I., Krátký, J., Havlica, J. & Brandštetr, J. (2014) Influence of superplasticizers on the course of Portland cement hydration, *Chemical Papers*, 68, 90–7, <https://doi.org/10.2478/s11696-013-0413-x>
- [35] Zeyad, A. M., Megat Johari, M. A., Tayeh, B. A. & Yusuf, M. O. (2016) Efficiency of treated and untreated palm oil fuel ash as a supplementary binder on engineering and fluid transport properties of high-strength concrete, *Construction and Building Materials*, 125, 1066–1079, <https://doi.org/10.1016/j.conbuildmat.2016.08.065>